Enhancing the radiative emission rate of single molecules by a plasmonic nanoantenna weakly coupled with a dielectric substrate

X. W. Chen,[1] K. G. Lee,[2,*] H. Eghlidi,[3] S. Götzinger,[4,5] and V. Sandoghdar[4,5]

[1]*School of Physics, Huazhong University of Science and Technology, 430074, Wuhan, China*
[2]*Department of Physics, Hanyang University, 222 Wangsimni-ro, Seongdong-gu, Seoul, 133-791, South Korea*
[3]*Laboratory of Thermodynamics in Emerging Technologies, ETH Zurich, 8092 Zurich, Switzerland*
[4]*Department of Physics, Friedrich-Alexander University Erlangen-Nürnberg, 91058 Erlangen, Germany*
[5]*Max Planck Institute for the Science of Light, 91058 Erlangen, Germany*
[*]*kglee@hanyang.ac.kr*

Abstract: Enhancing the spontaneous emission of single emitters has been an important subject in nano optics in the past decades. For this purpose, plasmonic nanoantennas have been proposed with enhancement factors typically larger than those achievable with optical cavities. However, the intrinsic ohmic losses of plasmonic structures also introduce an additional nonradiative decay channel, reducing the quantum yield. Here we report on experimental studies of a weakly coupled dielectric substrate and a plasmonic nanoantenna for enhancing the radiative decay rate of single terrylene molecules embedded in an ultrathin organic film. We systematically investigate how the refractive index of the dielectric substrate affects the lifetime and the quantum efficiency and show that the coupled structure could moderately enhance the radiative decay rate while maintaining a high quantum efficiency.

OCIS codes: (240.6680) Surface plasmons; (270.5580) Quantum electrodynamics; (240.6648) Surface dynamics.

References and links

1. K. Drexhage, "Interaction of light with monomolecular dye layers," Prog. Opt. **120**, 164–232 (1974).
2. P. R. Berman, *Cavity Quantum Electrodynamics* (Academic Press, 1994).
3. R. K. Chang and A. J. Campillo, eds., *Optical Processes in Microcavities* (World Scientific, 1996).
4. H. Yokoyama and K. Ujihara, eds., *Spontaneous Emission and Laser Oscillation in Microcavities* (CRC Press, 1995).
5. D. Press, S. Götzinger, S. Reitzenstein, C. Hofmann, A. Löffler, M. Kamp, A. Forchel, and Y. Yamamoto, "Photon antibunching from a single quantum-dot-microcavity system in the strong coupling regime," Phys. Rev. Lett. **98**(11), 117402 (2007).
6. J.-J. Greffet, "Applied physics. Nanoantennas for light emission," Science **308**(5728), 1561–1563 (2005).
7. M. Agio and A. Alù, *Optical Antennas* (Cambridge University Press, Cambridge, 2013).
8. X. W. Chen, M. Agio, and V. Sandoghdar, "Metallodielectric hybrid antennas for ultrastrong enhancement of spontaneous emission," Phys. Rev. Lett. **108**(23), 233001 (2012).
9. M. Frimmer and A. F. Koenderink, "Spontaneous emission control in a tunable hybrid photonic system," Phys. Rev. Lett. **110**(21), 217405 (2013).
10. F. Bigourdan, F. Marquier, J.-P. Hugonin, and J.-J. Greffet, "Design of highly efficient metallo-dielectric patch antennas for single-photon emission," Opt. Express **22**(3), 2337–2347 (2014).
11. T. Kalkbrenner, M. Ramstein, J. Mlynek, and V. Sandoghdar, "A single gold particle as a probe for apertureless scanning near-field optical microscopy," J. Microsc. **202**(1), 72–76 (2001).
12. A. Taflove and S. C. Hagness, *Computational Electrodynamics: The Finite-Difference Time-Domain Method*, 3rd ed. (Artech House, 2005).
13. R. J. Pfab, J. Zimmermann, C. Hettich, I. Gerhardt, A. Renn, and V. Sandoghdar, "Aligned terrylene molecules in a spin-coated ultrathin crystalline film of p-terphenyl," Chem. Phys. Lett. **387**(4-6), 490–495 (2004).
14. S. Kühn, U. Håkanson, L. Rogobete, and V. Sandoghdar, "Enhancement of single-molecule fluorescence using a gold nanoparticle as an optical nanoantenna," Phys. Rev. Lett. **97**(1), 017402 (2006).
15. H. Eghlidi, K. G. Lee, X. W. Chen, S. Götzinger, and V. Sandoghdar, "Resolution and enhancement in nanoantenna-based fluorescence microscopy," Nano Lett. **9**(12), 4007–4011 (2009).

#251761 Received 12 Oct 2015; revised 30 Nov 2015; accepted 30 Nov 2015; published 14 Dec 2015

16. M. Kreiter, M. Prummer, B. Hecht, and U. P. Wild, "Orientation dependence of fluorescence lifetimes near an interface," J. Chem. Phys. **117**(20), 9430–9433 (2002).
17. S. Kühn, G. Mori, M. Agio, and V. Sandoghdar, "Modification of single molecule fluorescence close to a nanostructure: radiation pattern, spontaneous emission and quenching," Mol. Phys. **106**(7), 893–908 (2008).
18. H. Cang, Y. Liu, Y. Wang, X. Yin, and X. Zhang, "Giant suppression of photobleaching for single molecule detection via the Purcell effect," Nano Lett. **13**(12), 5949–5953 (2013).
19. B. C. Buchler, T. Kalkbrenner, C. Hettich, and V. Sandoghdar, "Measuring the quantum efficiency of the optical emission of single radiating dipoles using a scanning mirror," Phys. Rev. Lett. **95**(6), 063003 (2005).
20. X. W. Chen, W. C. H. Choy, and S. He, "Efficient and rigorous modeling of light emission in planar multilayer organic light-emitting diodes," J. Disp. Technol. **3**(2), 110–117 (2007).
21. K. Koyama, M. Yoshita, M. Baba, T. Suemoto, and H. Akiyama, "High collection effieciency in fluorescence microscopy with a solid immersion lens," Appl. Phys. Lett. **75**(12), 1667–1669 (1999).

1. Introduction

Controlling the emission of single quantum emitters has been a topic of theoretical and experimental investigations over the past decades for fundamental studies and emerging applications. A single quantum emitter can produce a sequence of well-defined single photons when a proper excitation scheme is applied, for example, by exciting it with regular laser pulses. However, due to the small size of the transition dipole moment of optical emitters, the lifetime of the excited state is typically in the order of nanoseconds, which severely limits the emission rate of such kinds of single-photon sources. Starting with the pioneering work by Drexhage [1], various microcavity schemes have been extensively applied to control spontaneous emission (SE) [2–4]. In these approaches, the difficulties of obtaining high quality factors and small mode volumes restrict the attainable SE enhancement, so that the highest reported value is still under 100 [5]. Another technical challenge for cavities is that the emission linewidth of the emitters must be narrow enough to be efficiently coupled to the cavity modes. Therefore experiments with solid-state emitters have to be performed at low temperatures. Recent reports have shown that metallic nanoparticles can enhance the emission in analogy with antenna concepts from radio engineering [6, 7]. The SE rate in a broad spectral range can be manipulated in a well-controlled manner. However, due to the dissipation in the metal, it is difficult to achieve strong enhancement of the emission without invoking quenching.

To circumvent this problem, hybrid systems combining dielectric and metallic units have been suggested [8–10]. In these designs, the plasmonic structure is strongly coupled with the dielectric structure and thus one can obtain ultrastrong enhancements of the SE rate while maintaining a relatively high quantum efficiency (QE). Here we report on a metallo-dielectric antenna structure for modifying SE in a different regime, where the dielectric substrate and the plasmonic nanoantenna are weakly coupled. Here, the weak coupling refers to the relatively weak interaction between the plasmon resonance and the substrate. Compared to the cases in Ref [8], the shift of the plasmon resonance and the change of the decay rate are relatively small. In this case, each component of the hybrid antenna plays a clear role in modifying the emission process. By employing a near-field scanning optical microscopy platform [11], we quantitatively study how the SE rate of single terrylene molecules changes depending on the refractive index, n, of the substrate with/without coupling to a spherical plasmonic antenna. In particular, we observed that the SE rate increased roughly 1.5 times when n is increased from 1.52 (glass) to 2.2 (cubic-zirconia) and were further enhanced by another factor of 30 with a gold nanoparticle (GNP) nearby. In addition, the QE of the coupled antenna-molecule system increases with higher n. Calculations based on the body-of-revolution finite-difference time domain method (BOR-FDTD) [12] successfully reconstruct the experimental data.

2. Experiment

Figure 1 shows the schematics of our experimental arrangement. Terrylene molecules were embedded in a thin (~20 nm) *para*-Terphenyl (pT) crystal generated by a spin coating method [13] onto substrates with different refractive indices: n = 1.52 (glass), 1.78 (sapphire) and 2.2 (cubic zirconia). An excitation source consisting of a 532 nm pulsed laser with 13 ps pulse

#251761 Received 12 Oct 2015; revised 30 Nov 2015; accepted 30 Nov 2015; published 14 Dec 2015

width was coupled through the objectives in a total internal reflection configuration. The incident electric field was *p*-polarized for efficient coupling of the excitation light to molecules aligned almost vertically to the sample surface [13]. Fluorescence from the molecules was collected by the same objective and sent to a single-photon detector (id-Quantique, id100) with a time resolution of 65 ps. A 565-nm long-pass filter was used to eliminate the green excitation from the detection path. Oil objectives were used for the glass and sapphire cover slips. For the cubic zirconia substrate (n = 2.2), we used a solid immersion lens (SIL) combined with a high numerical aperture (NA = 0.75) air objective. The fluorescence lifetime of single molecules was measured (Becker & Hickl GmbH, SPC-130) with and without a gold nanoparticle (GNP). More experimental details can be found in Refs [14, 15].

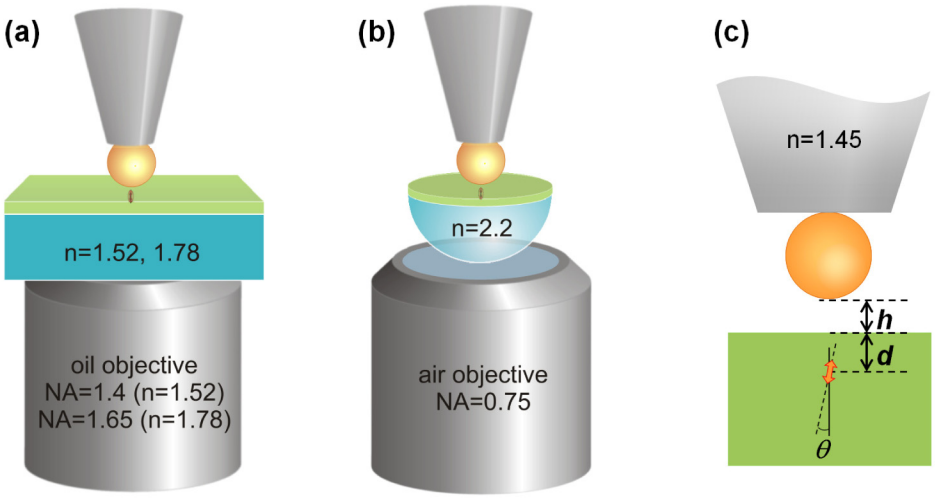

Fig. 1. Schematics of the experiment. (a, b) Substrate materials were glass, sapphire and cubic zirconia, with refractive indices of 1.52, 1.78, and 2.2, respectively. A thin film of pT embedding terrylene molecules was formed by spin coating onto the different substrates. The lifetime of the fluorescence from a single terrylene molecule was measured with and without the GNP approached to the molecule. A tapered glass fiber holding a GNP with diameter of 80 nm was placed close to a Terrylene molecule using shear-force feedback control. (c) System parameters used in the simulation, θ: tilting angle of terrylene molecule, d: molecule depth in pT crystal, h: separation between the bottom of the GNP and the pT top surface. The refractive index of the tip shaft is 1.45, and the apex size is 200 nm.

3. Results and discussion

Figure 2(a) shows the emission spectrum of a single terrylene molecule (red) at room temperature and the excitation laser wavelength (green). To identify the substrate-dependent trends, we performed experiments with many molecules for each substrate. The red circles in Fig. 2(b) show the measured lifetime of terrylene molecules in the absence of a plasmonic antenna. The spread of data points for each substrate mostly originates from the fact that each molecule has a different depth in the pT film. The experimentally measured lifetime of terrylene in a thick pT film is 4.0 ns, and it becomes longer in a thin pT film [16, 17], whereby the distance to the air interface determines the extent of this effect. The longest measured lifetime of terrylene in our experiment was 23.4 ns for the glass substrate. We note that molecules with longer lifetimes tend to be photo-bleached more easily possibly because they are more easily exposed to oxygen in the air [18]. Depending on the substrate, the fluorescence lifetime is reduced from about 20 ns (glass) to 11.6 ns (cubic zirconia) on average, confirming that the decay rate increases with an increase in n of the substrate. The decay of the emitter in excited state includes radiative decay channel and non-radiative decay channel. The ratio of the radiative decay to the total decay (the sum of the two channels) is

#251761 Received 12 Oct 2015; revised 30 Nov 2015; accepted 30 Nov 2015; published 14 Dec 2015

defined as the quantum efficiency. For molecules in pT film without coupled to a GNP, their quantum efficiencies are close to unity [19] and therefore their total decay rates are good approximation for the total decay rates. For molecules coupled to the GNP, as will be discussed later, both the radiative and nonradiative decay channels are enhanced.

To simulate the system, we applied a plane-wave decomposition method [20], where an oscillating current dipole is assumed and the radiated power is calculated and compared to a reference dipole in a homogenous host material ($1/\gamma_h^{rad} = \tau_h^{rad} = 4\ ns$). The QE of the terrylene molecule is assumed to be 96% [19]. The tilting angle θ shown in Fig. 1(c) is set to be 15 degrees and the refractive index of the pT film is assumed to be 1.9 [13]. Black lines in Fig. 2(b) show the calculated relative radiative decay rates for 4 different molecular depths d in the pT film. The black circles in Fig. 2(b) converted from the red circles represent the radiative decay rate with a reference value of 1 for molecules in bulk pT crystal. The overall trend in the calculation matches well with the experimental findings. In a nutshell, near fields of a single molecule contain a large distribution of k-vectors and the bottom substrate channels the emission in the range $k_0 < k < k_0 n$, where k_0 is the vacuum wave number. Larger n allows more coupling of emission into the substrate, enhancing the radiative decay rate.

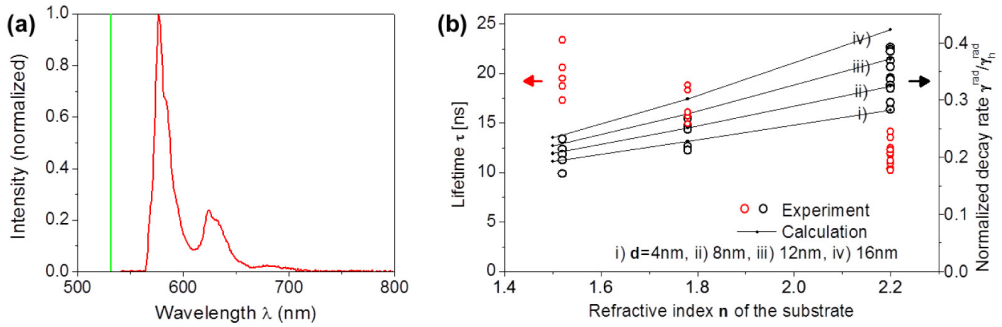

Fig. 2. (a) Emission spectrum of terrylene at room temperature (red) and the excitation laser wavelength (green). (b) Red circles are the fluorescence lifetime of single terrylene molecules in pT film formed on substrates with different n values, glass (n = 1.52), sapphire (1.78), and cubic Zirconia (2.2). Each circle represents data from a different molecule. Black circles are the inverse of the measured lifetiems, normalized to a reference (γ_h^{rad}) terrylene molecule in a homogeneous host material (pT) and compared to theoretical values in black lines.

When a plasmonic nano-antenna is approached to a molecule, the main factor governing the radiative decay rate becomes the plasmon resonance of the antenna although there is still a considerable contribution from the substrate. The fact that the terrylene molecules are oriented vertically provides a substantial advantage for the enhancement of the emission. A contour plot of the z-component (vertical) electric field enhancement is displayed in Fig. 3(a). The calculated enhancement factor is defined as the ratio of the field amplitude with GNP to the value without the GNP. One observes that due to the presence of the GNP the z-component of the electric field is greatly enhanced in the thin pT film. In this situation, to get a large enhancement on the decay rate, we carried out the measurements only for molecules placed close to the air-pT interface (molecules with long lifetime when they are not coupled to a GNP). In Fig. 3(b), it is shown, in a logarithmic scale, the fluorescence lifetimes of a terrylene molecule with (black line) and without (red line) coupled to a GNP on a glass substrate. The scattering resonance of a GNP 80 nm in diameter is shown in Fig. 3(c), and the calculated radiative decay rate curves in Fig. 3(d) follow the shape of the measured scattering resonance of the GNP. For metallic antennas, one should also take into account another important factor, the QE. As expected, the Ohmic losses become smaller at longer wavelengths, allowing for relatively higher QE, but at shorter wavelengths QE drops abruptly due to significant quenching effects. As shown in Fig. 3(e), the QE is higher with higher n

#251761 Received 12 Oct 2015; revised 30 Nov 2015; accepted 30 Nov 2015; published 14 Dec 2015

values of the substrate in the emission spectral range of terrylene molecules. To calculate the QE of the emitter for a given configuration, we computed using BOR-FDTD [12] the power radiated by the molecule (an electric dipole) into the far field as well as the total power dissipated (i.e., radiatively and nonradiatively) by the molecule and determined the ratio of the former to the latter.

To study this effects experimentally, we measured the lifetime of many terrylene molecules by approaching a single GNP with nanometer accuracy using a shear-force feedback. As shown in Fig. 3(f), the total decay rate reach about 10 times higher values than in bulk (see Fig. 2b). Figure 3(f) also shows that the theory agrees with the trend of the experimental data recorded as a function of n. Here, the inverse of the lifetime indicates the total decay rate, i.e., the radiative decay rate plus the non-radiative decay rate. To experimentally derive the quantum yield of the molecule coupled to a GNP, one needs to measure a saturation curve of the fluorescence while varying the excitation beam flux. In our work, however, molecules photo-bleached during the measurements. We could therefore not measure a saturation curve for all the data points. To this end, we theoretically calculated the quantum yield and the total decay rate to compare with experimentally measured total decay rates. Experimentally it was not possible to control the depth of molecule in the pT layer. We can nevertheless confirm the trend that the total decay rate increases with n. The values we obtain experimentally agree actually quite well with the calculated decay rates for the two refractive indices and various d (see Fig. 3(f)). Considering that the QE is expected to be higher for larger n (QE values for all theoretical data points in Fig. 3(f) are given in parentheses), we conclude that the radiative decay rate increases with n. In our experimental conditions, the distances between the substrate and the GNP were more than 5 nm and therefore the two were not strongly coupled as it can be observed from the small change of the plasmon spectrum shape shown in Fig. 3(d). Consequently, effects from each component of the hybrid antenna on the modification of the emission can be identified.

#251761 Received 12 Oct 2015; revised 30 Nov 2015; accepted 30 Nov 2015; published 14 Dec 2015

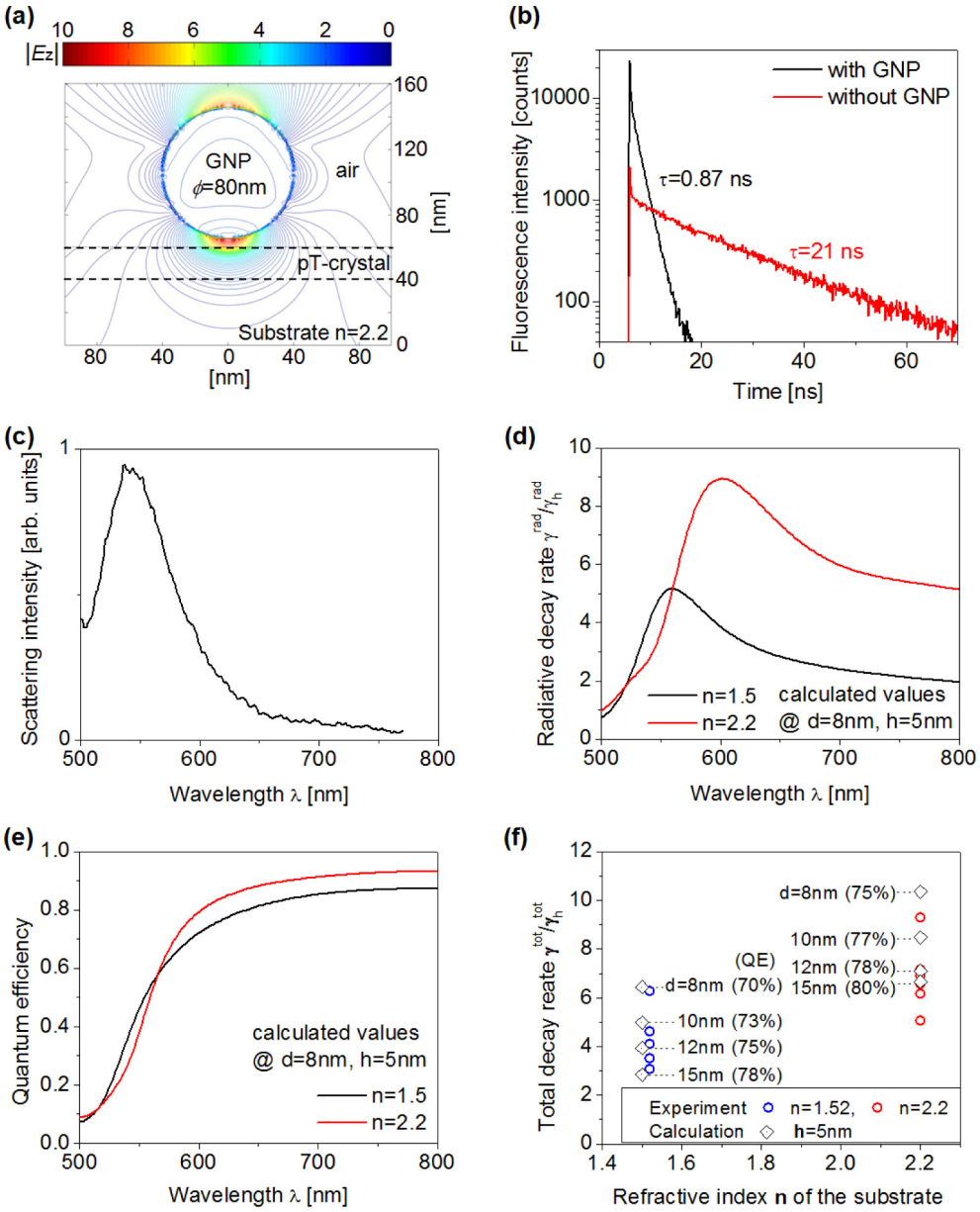

Fig. 3. (a) A contour plot of the *z*-component (vertical) electric field enhancement. It is shown the amplitude instead of the intensity for a better visualization. (b) Measured fluorescence lifetime of a terrylene molecule with (black) and without (red) coupled to a GNP for a glass substrate. (c) Measured scattering resonance of a GNP 80 nm in diameter. (d) Calculated radiative decay rate of an emitter embedded in the dielectric medium discussed in Fig. 1 in the presence of a GNP. The values are normalized to the reference case. (e) Calculated QE of the system with GNP as a function of the emission wavelength. (f) Normalized total decay rate. QE values are given in parentheses. For each substrate 5 ~6 different tips were used.

4. Conclusions

We studied how the SE rate of a single emitter is affected by the refractive index *n* of the substrate with and without a plasmonic optical antenna. When *n* is changed from 1.52 (glass) to 2.2 (cubic-zirconia), the emission rate increases by 1.5 times without GNP antenna. When

#251761 Received 12 Oct 2015; revised 30 Nov 2015; accepted 30 Nov 2015; published 14 Dec 2015

a plasmonic antenna consisting of an 80 nm spherical GNP is coupled to terrylene molecules, the SE rate is additionally enhanced by about 30 times regardless of the substrate index of refraction. This means that the absolute SE rate with a nano-antenna increases by the similar factor when the substrate index changes from 1.52 to 2.2. In other words, higher *n* values of the dielectric substrate allow larger radiative decay rates, both with and without a plasmonic antenna. In addition, substrates with higher *n* help to increase the collection efficiency of the fluorescence of single emitters [21].

Acknowledgments

This work was supported by the Max Planck Society, the Basic Science Research Program through the National Research Foundation of Korea funded by the Ministry of Science, ICT & Future Planning (2013R1A1A1011514), and the National Natural Science Foundation of China (NSFC, No. 11474114).

#251761 Received 12 Oct 2015; revised 30 Nov 2015; accepted 30 Nov 2015; published 14 Dec 2015